Electronic Supplementary Information

A nickel-iridium alloy as an efficient heterogeneous catalyst for hydrogenation of olefins

Jia-qi Bai, Masazumi Tamura,* Yoshinao Nakagawa, and Keiichi Tomishige*

Department of Applied Chemistry, Graduate School of Engineering, Tohoku University, 6-6-07 Aoba, Aramaki, Aoba-ku, Sendai 980-8579, Japan

Corresponding Authors

*E-mail: mtamura@erec.che.tohoku.ac.jp

*E-mail: tomi@erec.che.tohoku.ac.jp

1. General

The products were analyzed by GC (Shimadzu GC-2014) and GC-MS (Shimadzu QP-5050) with TC-WAX capillary column (GL Sciences Inc., diameter 0.25 mm, 30 m) for hydrogenation of styrene and hydrogenation of ethylbenzene or with PONA-J capillary column (Restek Corporation, diameter 0.25 mm, 100 m) for hydrogenation of 1-octene or hydrogenation of 2-octene. All chemicals were obtained from commercial suppliers and used without further purification. Styrene (FUJIFILM Wako Pure Chemical Corporation, >99%), ethylbenzene (FUJIFILM Wako Pure Chemical Corporation, >98%), 1-octene (FUJIFILM Wako Pure Chemical Corporation, >95%), 2-octene (*cis*- and *trans*-mixture, *trans*/*cis*=0.24, Tokyo Chemical Industry Co., Ltd., >98%), ethylcyclohexane (Sigma-Aldrich, >99%), methanol (Kanto Chemical Co., Inc. >99.8%), *n*-dodecane (Tokyo Chemical Industry Co., Ltd., >99%), ethanol (Kanto Chemical Co., Inc. >99.5%), *n*-octane (Tokyo Chemical Industry Co., Ltd., >97%), *cis*-4-octene (Tokyo Chemical Industry Co., Ltd., >95%), *trans*-4-octene (Tokyo Chemical Industry Co., Ltd., >99%), *trans*-3-octene (Tokyo Chemical Industry Co., Ltd., >98%).

2. Catalyst Preparation

All the catalysts were prepared by impregnation method. A typical preparation method for Ni-Ir/SiO_2 is as follows: Firstly, Ir/SiO_2 was synthesized by impregnating SiO_2 (Fuji Silysia Ltd., G-6, calcined at 973 K, 1 h) with H_2IrCl_6 aqueous solution (Furuya Metals Co., Ltd), then it was dried in oven at 373 K overnight after water evaporation. Ni was loaded on the Ir/SiO_2 by impregnating Ir/SiO_2 with $Ni(NO_3)_2$ (Wako Pure Chemical Industries, Ltd.) aqueous solution, followed by drying in oven at 373 K overnight after water evaporation. Finally, the obtained wet Ni-Ir/SiO_2 was calcinated at 773 K for 3 h in muffle furnace. Ni/SiO_2 was prepared by impregnating SiO_2 with $Ni(NO_3)_2$ aqueous solution in the same method. All catalysts were reduced under H_2 flow (30 ml/min) at 773, 1073 or 1173 K for 1 h just before use (as described below), and obtained catalysts were described as Ni-Ir/SiO_2-X (*T*), where X is the introduced Ni/Ir molar ratio and *T* is the reduction temperature (if not described, *T* is 773 K).

3. Typical Procedure for Hydrogenation of Styrene

Activity tests were conducted in a 190-ml stainless steel autoclave with an inserted glass vessel. The standard reaction conditions of hydrogenation of styrene are shown as follows: reduced catalyst (typically 20 mg), spinner and the mixture of styrene (200 mmol) and methanol (30 g) were added into the autoclave under air except for Ni/SiO_2. In order to avoid the oxidation of Ni metal species by exposing them to air, Ni/SiO_2 catalyst was transferred into the autoclave in glovebox with N_2. The air was purged by flushing with H_2 (1 MPa, 99.99%, Nippon Peroxide Co., Ltd.) three times after sealing the reactor. Then the autoclave was heated to 303 K and H_2 pressure was increased to 8 MPa and the stirring speed was fixed at 500 rpm (the mass transfer limitation was ruled out at 500 rpm, as shown in Table S8). The reaction temperature was monitored by a thermocouple inserted in the autoclave. After the reaction, the reactor was cooled to room temperature in water bath. The liquid phase was transferred to a vial and then washed by 10 g ethanol. The products were analyzed by GC with TC-WAX. Conversion of the styrene and selectivity of products were calculated by GC with *n*-dodecane (about 0.8 g) as an internal standard. TOF_s was calculated as follows: TOF_s (min^{-1}) = (Converted substrate (mmol))/(surface Ir and Ni metal amount (mmol))/(Time (min)). The surface Ir and Ni metal amount was calculated by integration of total metal amount with dispersion determined by H_2 adsorption. The qualitative analysis was conducted by GC-MS with TC-WAX. Reusability test of Ni-Ir/SiO_2-1 was conducted as follows: the catalyst was recovered from the reaction mixture by centrifugation. After washing with ethanol (20 g) and drying, the catalyst was directly reused for the next reaction under the same reaction conditions as the activity test.

The amount of isolated Ni amount is calculated on the basis of following assumptions, and the equation is shown in eq. 1.

1. All Ir metals are used for alloy formation.
2. Alloy surface is fcc (111).
3. Composition of Ni-Ir alloys is based on the results of XRD by using Vegard's law.
4. Ni-Ir Alloys are well-mixed ones.

Amount of isolated Ni amount (mmol g^{-1}) = (Surface Ni in Ni-Ir alloy (mmol g^{-1})) × $(1\text{-Ni}/(\text{Ni+Ir}))^6$ (eq. 1)

(1-Ni/(Ni+Ir)) represents the probability of the absence of Ni species around one Ni site, and the superscript 6 after (1-Ni/(Ni+Ir)) represents the number of metal sites around one certain Ni site. (surface Ni in Ni-Ir alloy (mmol g^{-1})) was calculated by assuming that the dispersion is 20% in Ni-Ir alloys as shown in eq. 2

Surface Ni in Ni-Ir alloy (mmol g^{-1}) = Ir amount (mmol g^{-1}) × A/(1-A) × 0.2 (eq. 2)

A is the alloy composition of Ni/(Ir+Ni) in Table 1.

4. Characterization

Temperature-programmed reduction (TPR) was carried out in a fixed-bed reactor equipped with a thermal conductivity detector using 5% H_2 diluted with Ar (30 mL/min). The amount of catalyst was about 0.05 g (0.1 g for Ni/SiO_2(Ni=1.2wt%)), and the temperature was increased from room temperature to 1073 K at a heating rate of 10 K/min.

X-ray diffraction (XRD) patterns were recorded by a diffractometer (MiniFlex600, Rigaku). Cu *K*α (λ = 0.154 nm, 45 kV, 40 mA) radiation was used as an X-ray source. In order to precisely obtain the position of XRD peaks, the sample was mixed with Si powder for measurement and XRD patterns were calibrated with Si (111) of 28.42°. The average metal particle size was estimated using Scherrer's equation.

Field emission scanning transmission electron microscope (FE-STEM) images and energy-dispersive X-ray (EDX) analyses were obtained by a Hitachi spherical aberration corrected STEM/SEM HD-2700 instrument operated at 200 kV. After the reduction and passivation, the samples were dispersed in ethanol and placed on Cu grids under air atmosphere. Average particle size was calculated by $\sum n_i d_i^3 / \sum n_i d_i^2$($d_i$, particle size; n_i, number of particles with d_i) and Ni/Ir ratio was obtained based on Cliff Lorimer method.

The amount of H_2 adsorption was measured in a high-vacuum system using a volumetric method. The catalyst (~0.1 g) in the measurement cell was reduced with H_2 at 773 K for 1 h and evacuated at 773 K for 1 h. After cooling, the adsorption amount of H_2 was measured at room temperature. Gas pressure at adsorption equilibrium was about 1.1 kPa. The dead volume of the apparatus was 42.48 cm^3. H_{total} was calculated based on the H atom amount of total adsorbed H_2 amount (sum of physical and chemical adsorption).

The amount of leached metals (Ir and Ni) into the reaction solution was analyzed by inductively coupled plasma atomic emission spectroscopy (ICP-AES, Thermo Fisher Scientific iCAP 6500).

The surface area of catalyst was measured with BET method (N_2 adsorption) using Shimadzu Gemini VII 2390a (Micromeritics).

X-ray absorption spectroscopy (XAS) was conducted at the BL01B1 station at SPring-8 with the approval of the Japan Synchrotron Radiation Research Institute (JASRI; Proposal No. 2018B1805). The storage ring was operated at 8 GeV, and a Si (111) single crystal was used to obtain a monochromatic X-ray beam. Two ion chambers for I_0 and I were filled with 85% N_2+15% Ar and 50% N_2+50% Ar, respectively, for Ir L_3-edge measurement. Two ion chambers for I_0 and I were filled with 100% N_2 and 15% N_2+85% Ar, respectively, for Ni K-edge measurement. The sample after the reduction and reaction were used for measurement. The calcinated Ni-Ir/SiO_2-1 (152.6 mg) was pressed into self-supporting disk with 10 mm diameter and reduced at 773 K for 1 h under H_2 for the sample after reduction, and then it was transferred to a measurement cell using a glove box filled with N_2. The catalytic reaction was conducted in the autoclave under the same reaction conditions as the standard reaction conditions for the sample after reaction, and, the autoclave was also transferred to glove box and the catalyst was transferred to a measurement cell after drying with thickness of 2 mm. The thickness of the cell filled with the powder was adjusted to give an edge jump of 0.2−1 for Ir L_3-edge and Ni K-edge measurement. The EXAFS data was collected by transmission mode for Ir L_3-edge and fluorescence mode for Ni K-edge. For EXAFS analysis, the oscillation was first extracted from the EXAFS data using a spline smoothing method.[1] Fourier transformation of the k^3-weighted EXAFS oscillation from the k space to the r space was performed to obtain a radial distribution function. The inversely Fourier filtered data were analyzed using a usual curve fitting method.[2] For curve fitting analysis, the empirical phase shift and amplitude function for the Ir−Ir bond and Ni-Ni bond were extracted from the data for Ir powder and Ni foil.

Theoretical functions for Ir-Ni bond and Ni-Ir bond were calculated by the FEFE8.2 program.[3] Analyses of EXAFS and XANES data were performed using a computer program (REX2000, ver. 2.6.0; Rigaku Corporation). Error bars for each parameter was estimated by stepping each parameter, while optimizing the other parameters, until the residual factor becomes 2 times than its minimum value.[4]

5. Supporting Figures and Tables

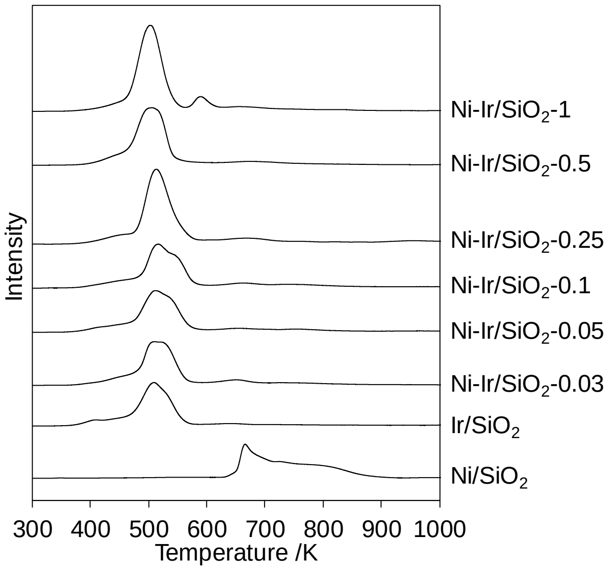

Figure S1. TPR profiles of various catalysts (Ni-Ir/SiO_2 (Ni/Ir=1, 0.5, 0.25, 0.1, 0.05, 0.03), Ir/SiO_2 (4wt%) and Ni/SiO_2 (1.2wt%)).

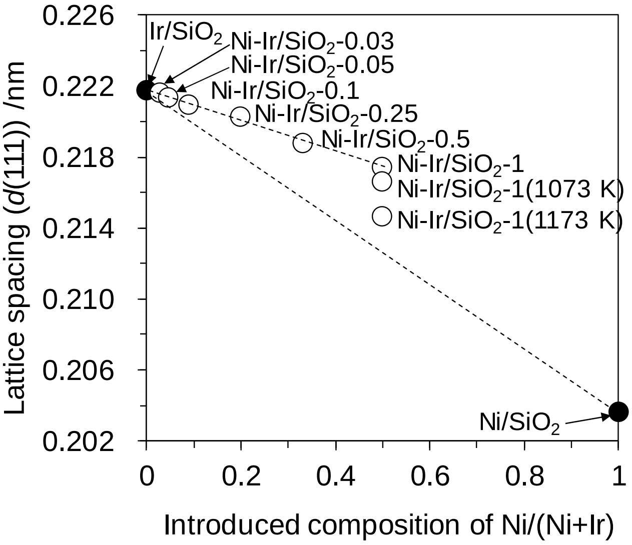

Figure S2. Relationship between the lattice spacing and introduced composition of Ni/(Ir+Ni)

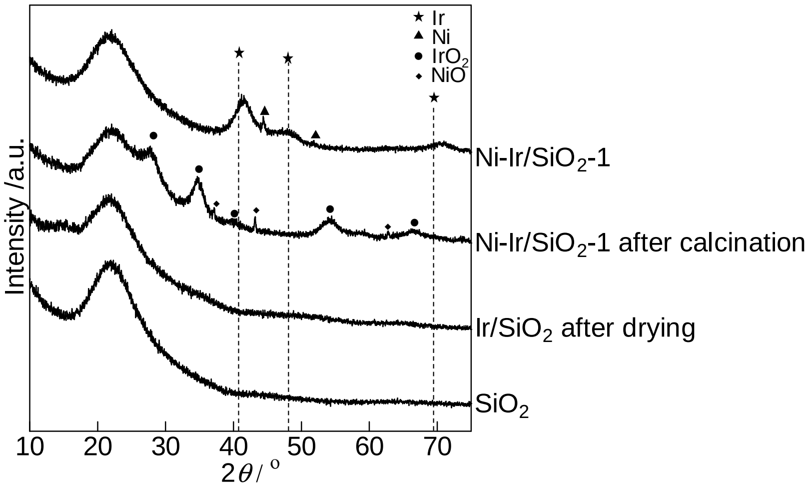

Figure S3. XRD patterns of SiO_2, Ir/SiO_2 after drying (before calcination), Ni-Ir/SiO_2-1 after calcination (before reduction), and Ni-Ir/SiO_2-1.

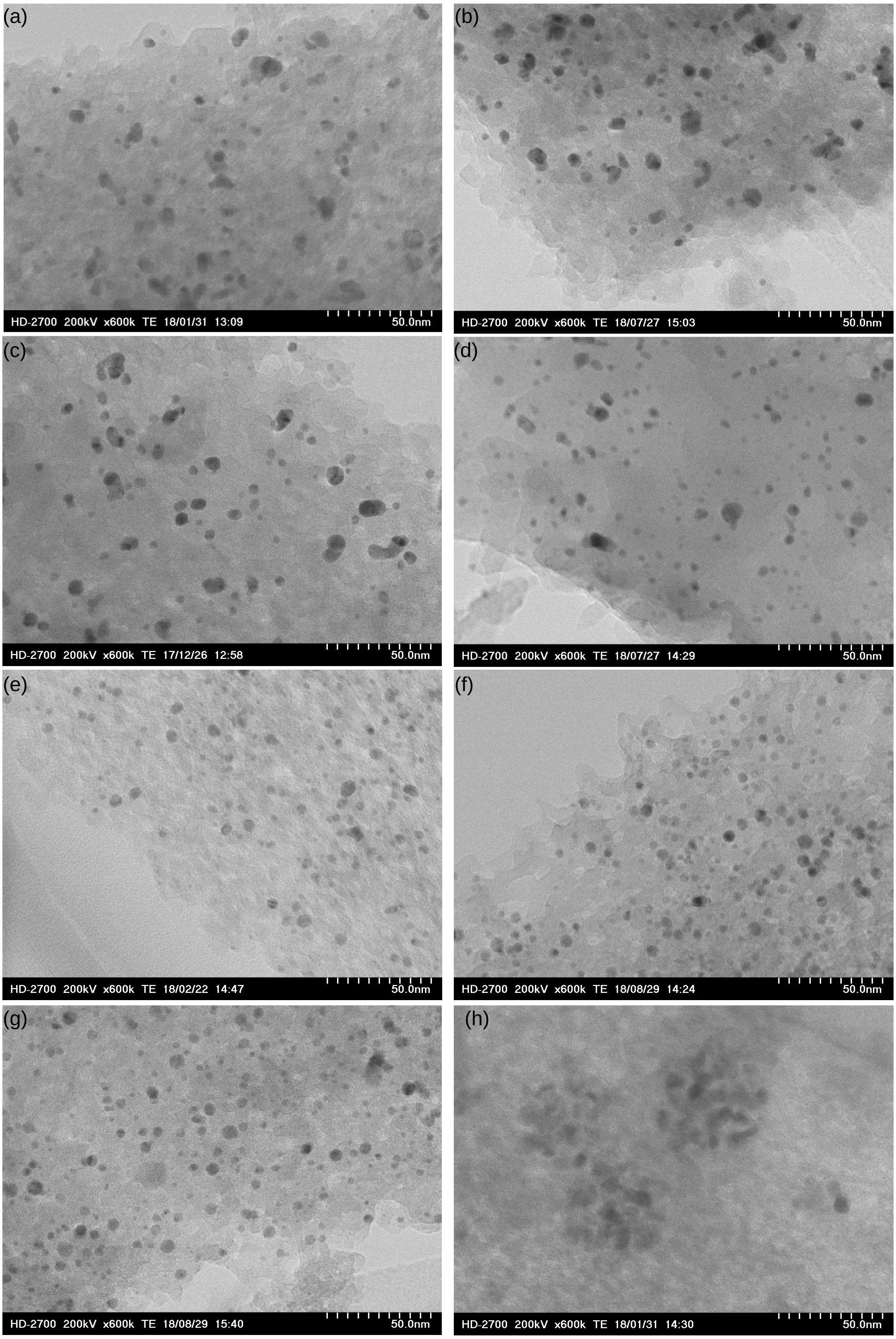

Figure S4. TEM analyses of Ni-Ir/SiO_2 catalysts

(a) Ir/SiO_2, (b) Ni-Ir/SiO_2-0.05, (c) Ni-Ir/SiO_2-0.1, (d) Ni-Ir/SiO_2-0.5, (e) Ni-Ir/SiO_2-1, (f) Ni-Ir/SiO_2-1 (1073 K), (g) Ni-Ir/SiO_2-1 (1173 K), (h) Ni/SiO_2.

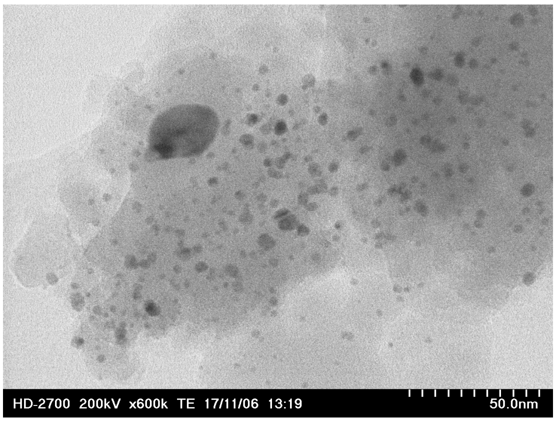

Figure S5. TEM analyses of Ni-Ir/SiO_2-1 catalyst with a large Ni particle.

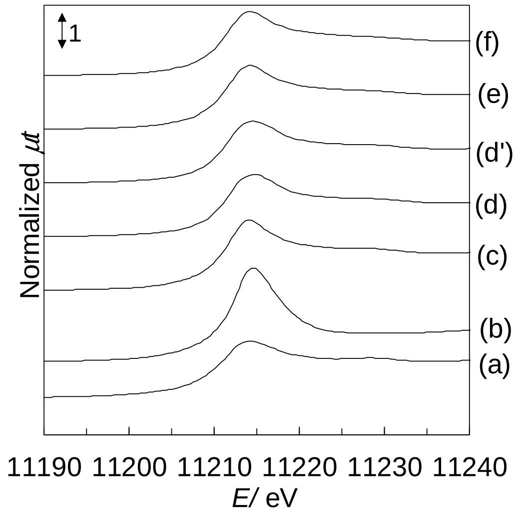

Figure S6. Ir L_3-edge XANES spectra of Ni-Ir/SiO_2-0.5, Ni-Ir/SiO_2-1 catalysts and related compounds. (a) Ir powder, (b) IrO_2, (c) Ni-Ir/SiO_2-0.5 after reduction, (d) Ni-Ir/SiO_2-1 after reduction, (d') Ni-Ir/SiO_2-1 after reaction, (e) Ni-Ir/SiO_2-1(1073 K) after reduction, (f) Ni-Ir/SiO_2-1(1173 K) after reduction.

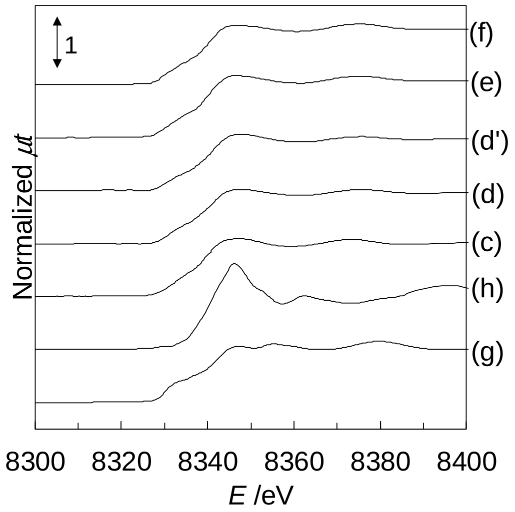

Figure S7. Ni *K*-edge XANES spectra of Ni-Ir/SiO_2-0.5, Ni-Ir/SiO_2-1 catalysts and related compounds (g) Ni foil, (h) NiO, (c) Ni-Ir/SiO_2-0.5 after reduction, (d) Ni-Ir/SiO_2-1 after reduction, (d') Ni-Ir/SiO_2-1 after reaction, (e) Ni-Ir/SiO_2-1(1073 K) after reduction, (f) Ni-Ir/SiO_2-1(1173 K) after reduction.

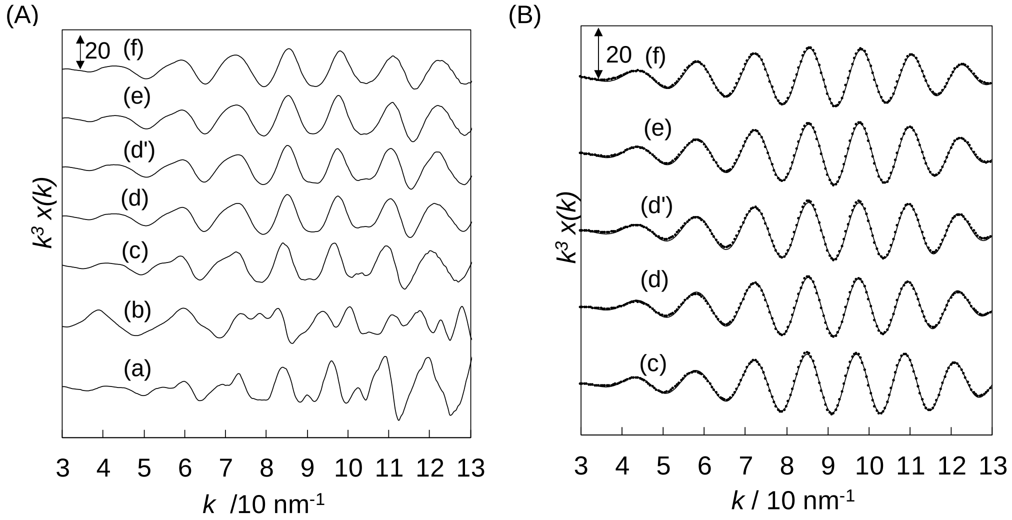

Figure S8. (A) k^3-weighted Ir L_3-edge EXAFS oscillations. (B) Fourier filtered Ir L_3-edge EXAFS data (solid line) and calculated data (dotted line). Fourier filtering range: 0.168-0.322 nm. (a) Ir powder, (b) IrO_2, (c) Ni-Ir/SiO_2-0.5 after reduction, (d) Ni-Ir/SiO_2-1 after reduction, (d') Ni-Ir/SiO_2-1 after reaction, (e) Ni-Ir/SiO_2-1(1073 K) after reduction, (f) Ni-Ir/SiO_2-1(1173 K) after reduction.

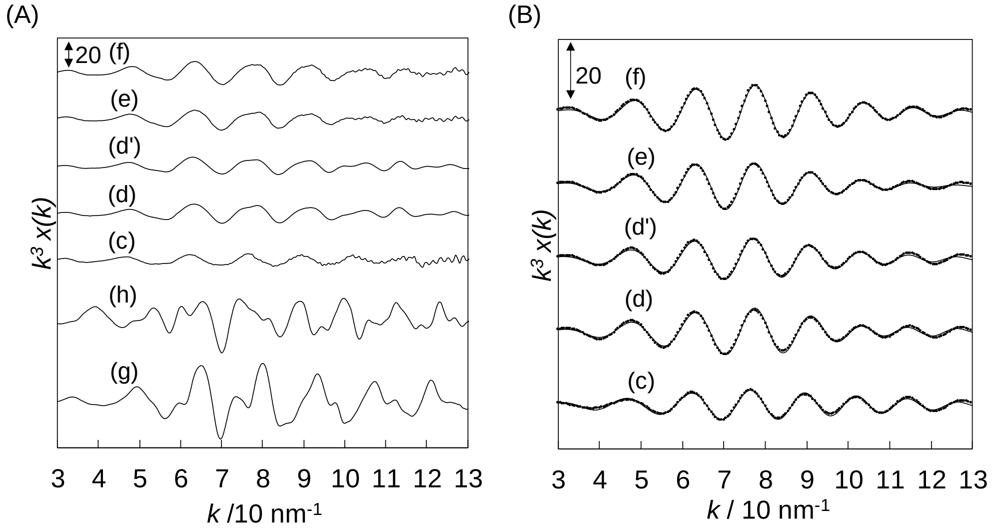

Figure S9. (A) k^3-weighted Ni K-edge EXAFS oscillations. (B) Fourier filtered Ni K-edge EXAFS data (solid line) and calculated data (dotted line). Fourier filtering range: 0.15-0.298 nm. (g) Ni foil, (h) NiO, (c) Ni-Ir/SiO_2-0.5 after reduction, (d) Ni-Ir/SiO_2-1 after reduction, (d') Ni-Ir/SiO_2-1 after reaction, (e) Ni-Ir/SiO_2-1(1073 K) after reduction, (f) Ni-Ir/SiO_2-1(1173 K) after reduction.

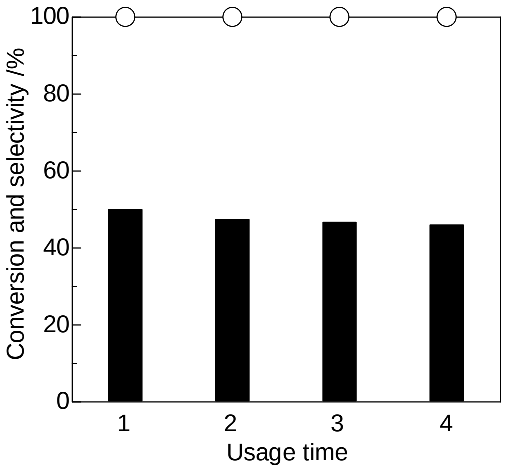

Figure S10. Reusability test of Ni-Ir/SiO_2-1 catalyst in hydrogenation of styrene

Black bar: conversion. ○: selectivity to ethylbenzene.

Reaction conditions: Ni-Ir/SiO_2-1 20 mg, styrene 200 mmol, methanol 30 g, H_2 8 MPa, 303 K, 0.5 h.

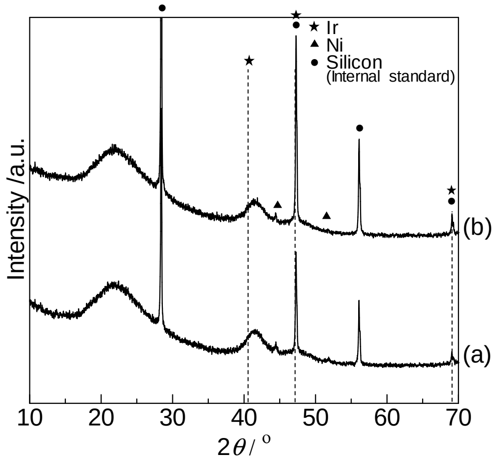

Figure S11. XRD profiles of (a) Ni-Ir/SiO_2-1 after reduction, (b) Ni-Ir/SiO_2-1 after reaction

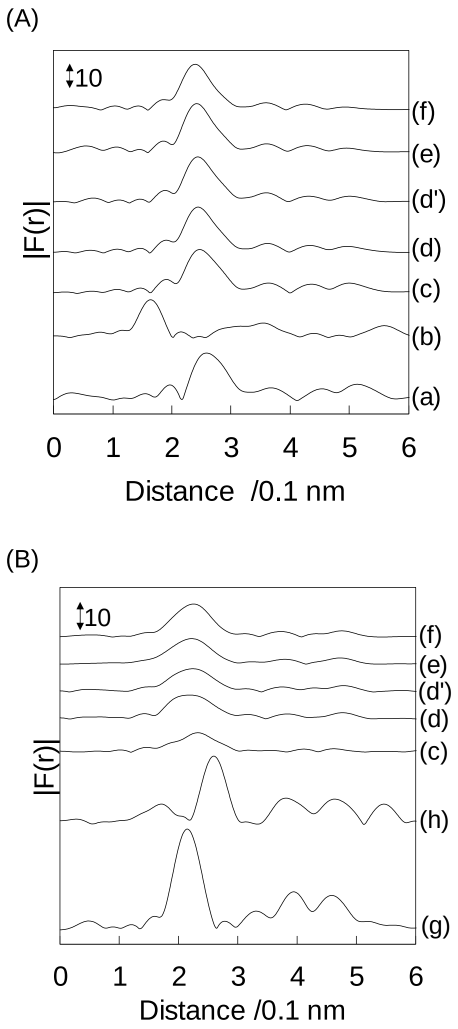

Figure S12. XAS analyses of Ni-Ir/SiO_2-0.5, Ni-Ir/SiO_2-1, Ni-Ir/SiO_2-1(1073 K), Ni-Ir/SiO_2-1(1173 K) catalysts and related compounds. (A) FT of k^3-weighted Ir L_3-edge EXAFS, FT range 30-130 nm^{-1}. (a) Ir powder, (b) IrO_2, (c) Ni-Ir/SiO_2-0.5 after reduction, (d) Ni-Ir/SiO_2-1 after reduction, (d') Ni-Ir/SiO_2-1 after reaction, (e) Ni-Ir/SiO_2-1(1073 K) after reduction, (f) Ni-Ir/SiO_2-1(1173 K) after reduction. (B) FT of k^3-weighted Ni K-edge EXAFS, FT range 30-130 nm^{-1}. (c) Ni-Ir/SiO_2-0.5 after reduction, (d) Ni-Ir/SiO_2-1 after reduction, (d') Ni-Ir/SiO_2-1 after reaction, (e) Ni-Ir/SiO_2-1(1073 K) after reduction, (f) Ni-Ir/SiO_2-1(1173 K) after reduction, (g) Ni foil, (h) NiO.

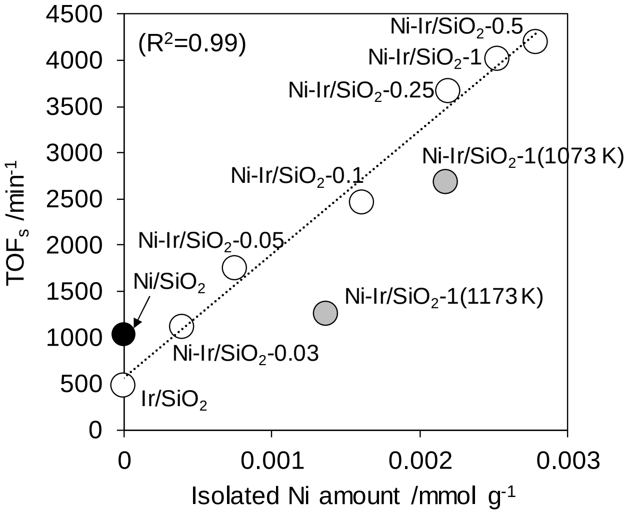

Figure S13. The correlation between TOF$_s$ and isolated Ni amount

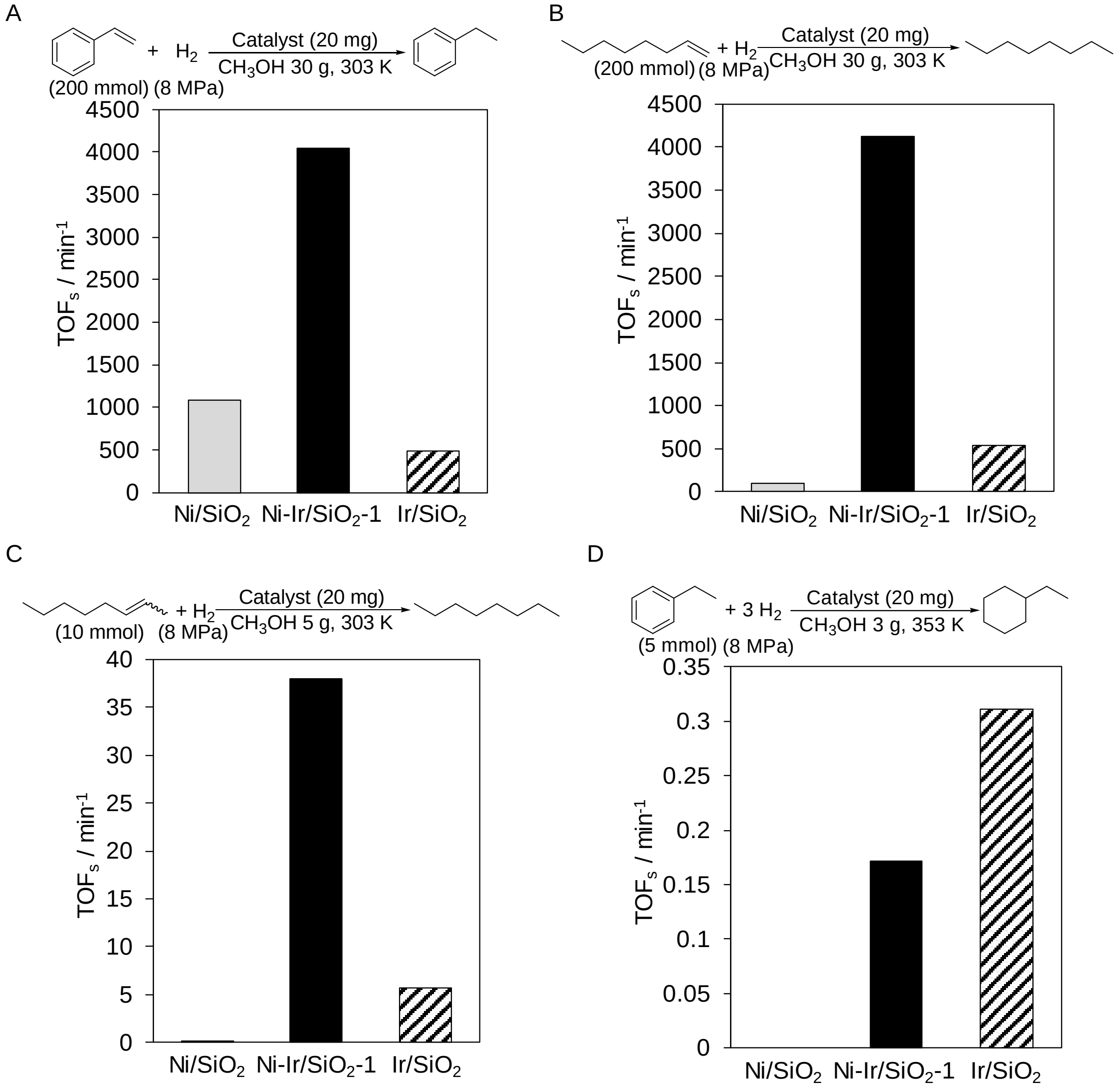

Figure S14. Activity comparison in hydrogenation of various substrates over Ni-Ir/SiO_2-1, Ni/SiO_2 and Ir/SiO_2 catalysts.

Table S1. H_2 consumption amount and reduction degree for Ir/SiO_2, Ni/SiO_2 and Ni-Ir/SiO_2 by TPR

Catalyst	Ni/Ir molar ratio	Used amount (mg)	Ir loading amount ($\times 10^{-5}$ mol)	Ni loading amount ($\times 10^{-5}$ mol)	H_2 consumption ($\times 10^{-5}$ mol)	Reduction degree		
						Ir	Ni	Total reduction degree (Ir+Ni)
Ir/SiO_2	0	54.6	1.13	0	2.38	1.0	-	1.1
Ni-Ir/SiO_2-0.03	0.03	55.1	1.15	0.04	2.54	1.0	(7.0)	1.1
Ni-Ir/SiO_2-0.05	0.05	55.5	1.15	0.06	2.51	1.0	(3.4)	1.1
Ni-Ir/SiO_2-0.1	0.1	52.8	1.10	0.11	2.43	1.0	(2.1)	1.1
Ni-Ir/SiO_2-0.25	0.25	54.7	1.14	0.29	2.84	1.0	(2.0)	1.1
Ni-Ir/SiO_2-0.5	0.5	53.1	1.13	0.57	2.88	1.0	1.1	1.1
Ni-Ir/SiO_2-1	1	53.4	1.11	1.11	3.60	1.0	1.2	1.1
Ni/SiO_2 (1.2 wt%)	-	98.0	0	2.04	2.11	-	1.0	1.0

The reduction degree of Ir and Ni species was calculated by assuming the following reaction formula:

$IrO_2 + 2H_2 \rightarrow Ir + 2H_2O$, $NiO + H_2 \rightarrow Ni + H_2O$.

The reduction degree of Ir species was assumed as 1.

Reduction degree (Ni) = ((H_2 consumption (mol)) – (Ir loading amount (mol))×2) / (Ni loading amount (mol))

Total reduction degree = (H_2 consumption (mol)) / ((Ir loading amount (mol))×2 + (Ni loading amount (mol)))

Table S2. Curve fitting results of Ir L_3-edge EXAFS of Ni−Ir/SiO$_2$-0.5, Ni−Ir/SiO$_2$-1, Ni−Ir/SiO$_2$-1(1073 K) and Ni−Ir/SiO$_2$-1(1173 K) catalysts

Catalyst	Condition	Shells	CN[a]	R / 10^{-1} nm[b]	σ / 10^{-1} nm[c]	ΔE_0 / eV[d]	R_f / %[e]
Ni-Ir/SiO$_2$-0.5	after reduction	Ir-Ir	9.6 ± 1.7	2.74 ± 0.01	0.056 ± 0.006	-2.3 ± 2.1	0.2
		Ir-Ni	1.8 ± 0.5	2.59 ± 0.01	0.065 ± 0.012	8.9 ± 4.7	
Ni-Ir/SiO$_2$-1	after reduction	Ir-Ir	8.9 ± 0.5	2.73 ± 0.01	0.064 ± 0.003	-3.6 ± 1.2	0.3
		Ir-Ni	2.4 ± 0.4	2.59 ± 0.01	0.066 ± 0.003	9.9 ± 2.0	
Ni−Ir/SiO$_2$-1	after reaction	Ir-Ir	8.9 ± 0.7	2.72 ± 0.01	0.064 ± 0.004	-3.8 ± 1.6	0.4
		Ir-Ni	2.4 ± 0.4	2.59 ± 0.01	0.067 ± 0.010	9.8 ± 2.0	
Ni−Ir/SiO$_2$-1(1073 K)	after reduction	Ir-Ir	8.4 ± 0.6	2.72 ± 0.01	0.064 ± 0.003	-1.1 ± 1.0	0.2
		Ir-Ni	3.2 ± 0.3	2.60 ± 0.01	0.067 ± 0.007	10.6 ± 1.4	
Ni−Ir/SiO$_2$-1(1173 K)	after reduction	Ir-Ir	7.5 ± 0.4	2.71 ± 0.01	0.066 ± 0.002	-3.9 ± 0.9	0.1
		Ir-Ni	4.2 ± 0.2	2.58 ± 0.01	0.079 ± 0.003	9.4 ± 0.8	
Ir powder	-	Ir−Ir	12	2.77	0.06	0	–

[a]Coordination number. [b]Bond distance. [c]Debye-Waller factor. [d]Difference in the origin of photoelectron energy between the reference and the sample. [e]Residual factor. Fourier filtering range: 0.168–0.322 nm.

Table S3. Curve fitting results of Ni K-edge EXAFS of Ni−Ir/SiO$_2$-0.5, Ni−Ir/SiO$_2$-1, Ni−Ir/SiO$_2$-1(1073 K) and Ni−Ir/SiO$_2$-1(1173 K) catalysts

Catalyst	Condition	Shells	CN[a]	R / 10^{-1} nm[b]	σ / 10^{-1} nm[c]	ΔE_0 / eV[d]	R_f / %[e]
Ni-Ir/SiO$_2$-0.5	after reduction	Ni−Ni	2.0	2.53	0.100	-9.7	2.5
		Ni−Ir	3.9	2.58	0.083	-10.5	
Ni-Ir/SiO$_2$-1	after reduction	Ni−Ni	5.8	2.50	0.099	-7.8	1.6
		Ni−Ir	2.4	2.60	0.071	0.5	
Ni−Ir/SiO$_2$-1	after reaction	Ni−Ni	5.8	2.52	0.104	-3.2	1.6
		Ni−Ir	2.4	2.60	0.074	-1.0	
Ni−Ir/SiO$_2$-1(1073 K)	after reduction	Ni−Ni	5.1	2.51	0.095	-8.4	0.8
		Ni−Ir	3.1	2.60	0.083	-5.2	
Ni−Ir/SiO$_2$-1(1173 K)	after reduction	Ni−Ni	5.5	2.52	0.088	-2.2	0.3
		Ni−Ir	4.2	2.59	0.085	-0.5	
Ni foil		Ni−Ni	12	2.49	0.06	0	–

[a]Coordination number. [b]Bond distance. [c]Debye-Waller factor. [d]Difference in the origin of photoelectron energy between the reference and the sample. [e]Residual factor. Fourier filtering range: 0.150–0.298 nm.

Table S4. H_2 adsorption of various catalysts and dispersion

Catalyst	Amount /g	Ni+Ir /mmol g^{-1}	H_{total} /mmol g^{-1}	Dispersion (H_{total}/(Ni+Ir)) /%
Ir/SiO_2	0.102	0.208	0.0460	22.0
Ni-Ir/SiO_2-0.03	0.106	0.213	0.0383	17.9
Ni-Ir/SiO_2-0.05	0.106	0.219	0.0370	16.9
Ni-Ir/SiO_2-0.1	0.108	0.229	0.0394	17.2
Ni-Ir/SiO_2-0.25	0.110	0.261	0.0313	12.0
Ni-Ir/SiO_2-0.5	0.105	0.311	0.0346	11.0
Ni-Ir/SiO_2-1	0.106	0.415	0.0392	9.5
Ni-Ir/SiO_2-1(1073 K)[a]	0.114	0.417	0.0398	9.6
Ni-Ir/SiO_2-1(1173 K)[a]	0.111	0.415	0.0251	6.1
Ni/SiO_2 (Ni=1.2 wt%)	0.104	0.208	0.0200	9.7

[a] The number in the parentheses is catalyst pre-reduction temperature.

Table S5. Time-courses over Ni-Ir/SiO$_2$ catalysts with various Ni loading amounts and reaction rates

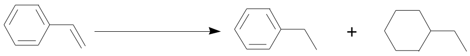

1 2

Catalyst	Dispersion /%	*t* /h	Conv. /%	Sel./% 1	Sel./% 2	Sel./% Others[b]	TOF$_s$ / min^{-1}
Ir/SiO$_2$	22.0	0	0	-	-	-	480
		0.25	3.5	98.5	1.1	0.4	
		0.5	6.5	98.5	1.1	0.4	
		1	13.1	98.2	1.3	0.5	
Ni-Ir/SiO$_2$-0.03	17.9	0	0	-	-	-	1110
		0.25	6.5	99.5	0.4	0.1	
		0.5	12.8	99.6	0.3	0.1	
Ni-Ir/SiO$_2$-0.05	16.9	0	0	-	-	-	1750
		0.08	3.2	99.8	0.2	<0.1	
		0.25	9.1	99.9	0.1	<0.1	
		0.5	19.7	99.9	0.1	<0.1	
Ni-Ir/SiO$_2$-0.1	17.2	0	0	-	-	-	2450
		0.08	4.5	>99.9	<0.1	<0.1	
		0.25	13.7	>99.9	<0.1	<0.1	
		0.5	29.4	>99.9	<0.1	<0.1	
Ni-Ir/SiO$_2$-0.25	12.0	0	0	-	-	-	3660
		0.08	5.4	>99.9	<0.1	<0.1	
		0.25	18.2	>99.9	<0.1	<0.1	
		0.5	33.8	>99.9	<0.1	<0.1	
Ni-Ir/SiO$_2$-0.5	11.0	0	0	-	-	-	4190
		0.08	6.3	99.9	<0.1	<0.1	
		0.25	22.1	99.9	<0.1	<0.1	
Ni-Ir/SiO$_2$-1	9.5	0	0	-	-	-	4000
		0.08	7.5	>99.9	<0.1	<0.1	
		0.17	16.1	>99.9	<0.1	<0.1	
		0.25	23.8	>99.9	<0.1	<0.1	
Ni-Ir/SiO$_2$-1 (1073 K)[a]	9.6	0	0	-	-	-	2680
		0.08	5.3	>99.9	<0.1	<0.1	
		0.25	16.0	>99.9	<0.1	<0.1	
Ni-Ir/SiO$_2$-1 (1173 K)[a]	6.1	0	0	-	-	-	1260
		0.08	5.0	>99.9	<0.1	<0.1	
		0.25	9.5	>99.9	<0.1	<0.1	

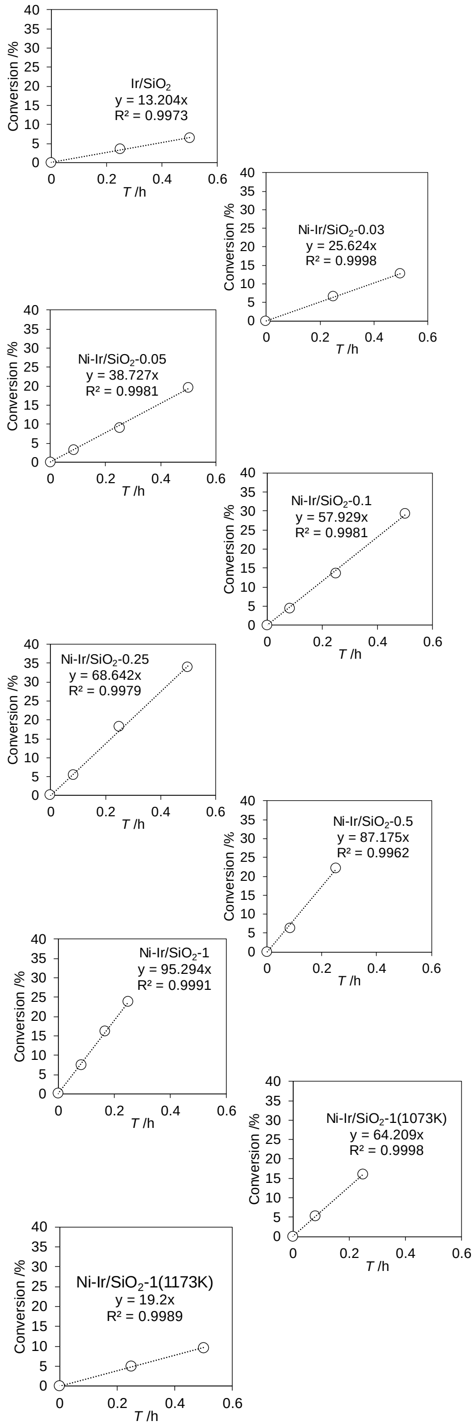

Reaction conditions: catalyst 20 mg, styrene 200 mmol, methanol 30 g, H$_2$ 8 MPa, 303 K.

[a] The number in the parentheses is catalyst pre-reduction temperature.

[b] Others include 1-ethylcyclohexene and other partial hydrogenation products of styrene hydrogenation.

Table S6. Calculated isolated Ni amount and TOF_s of various Ni-Ir/SiO_2 catalysts.

Catalyst	Alloy composition of Ni/(Ir+Ni)[b] /%	Calculated isolated Ni amount /mmol g^{-1}	TOF_s /min^{-1}
Ir/SiO_2	0	0	480
Ni-Ir/SiO_2-0.03	1	0.00040	1110
Ni-Ir/SiO_2-0.05	2	0.00075	1750
Ni-Ir/SiO_2-0.1	5	0.00161	2450
Ni-Ir/SiO_2-0.25	8	0.00219	3660
Ni-Ir/SiO_2-0.5	16	0.00278	4190
Ni-Ir/SiO_2-1	24	0.00253	4000
Ni-Ir/SiO_2-1(1073 K)[a]	29	0.00218	2680
Ni-Ir/SiO_2-1(1173 K)[a]	39	0.00137	1260
Ni/SiO_2 (Ni=1.2 wt%)	-	0	1030

[a] The number in the parentheses is catalyst pre-reduction temperature.

[b] Determined by XRD analyses based on Vegard's law.

The calculation method is described in the experimental in page S4.

Table S7. Results of hydrogenation of various substrates over Ni-Ir/SiO$_2$-1, Ni/SiO$_2$ and Ir/SiO$_2$ catalysts

(A) Hydrogenation of styrene

Catalyst	*t*	Conv.	Sel./%			TOF$_s$
	/h	/%	Ethylbenzene	Ethylcyclohexane	others[a]	/ min^{-1}
Ir/SiO$_2$	0	0	-	-	-	480
	0.25	3.5	98.5	1.1	0.4	
	0.5	6.5	98.5	1.1	0.4	
	1	13.1	98.2	1.3	0.5	
	2	25.4	97.6	1.6	0.8	
Ni-Ir/SiO$_2$-1	0	0	-	-	-	4000
	0.08	7.5	>99.9	<0.1	<0.1	
	0.17	16.1	>99.9	<0.1	<0.1	
	0.25	23.8	>99.9	<0.1	<0.1	
	0.5	47.8	>99.9	<0.1	<0.1	
	1	82.4	>99.9	<0.1	<0.1	
	2	100.0	>99.9	<0.1	<0.1	
Ni/SiO$_2$	0	0	-	-	-	1030
	0.25	3.3	>99.9	<0.1	<0.1	
	0.5	6.0	>99.9	<0.1	<0.1	
	1	13.5	>99.9	<0.1	<0.1	
	2	25.0	>99.9	<0.1	<0.1	

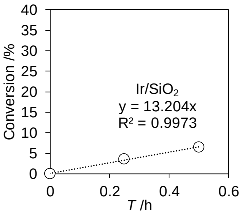

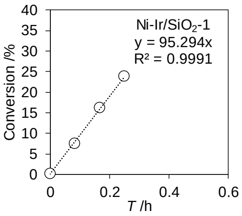

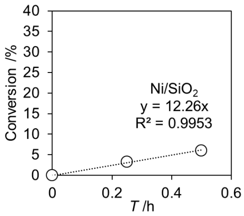

Reaction conditions: catalyst 20 mg, styrene 200 mmol, methanol 30 g, H$_2$ 8 MPa, 303 K.

[a]Others include 1-ethylcyclohexene and other partial hydrogenation products of styrene hydrogenation.

(B) Hydrogenation of 1-octene

Catalyst	*t*	Conv.	Sel./%			TOF$_s$
	/h	/%	*n*-Octane	*trans*-2-Octene	*cis*-2-Octene	/ min^{-1}
Ir/SiO$_2$	0	0	-	-	-	540
	0.25	3.3	>99.9	<0.1	<0.1	
	0.5	7.2	>99.9	<0.1	<0.1	
Ni-Ir/SiO$_2$-1	0	0	-	-	-	4100
	0.08	7.4	97.0	1.8	1.2	
	0.17	17.3	97.2	1.8	1.0	
Ni/SiO$_2$	0	0	-	-	-	94
	1	1.2	92.1	5.5	2.4	
	2	2.4	92.0	5.3	2.7	

Reaction conditions: catalyst 20 mg, 1-octene 200 mmol, methanol 30 g, H$_2$ 8 MPa, 303 K.

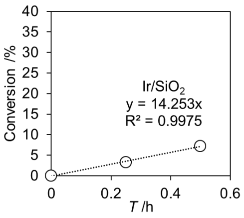

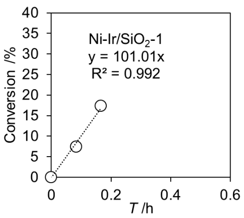

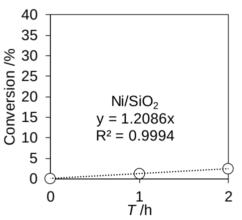

(C) Hydrogenation of 2-octene

Catalyst	*t* /h	Conv. /%	Sel./% *n*-Octane	Sel./% 3-Octene+4-Octene	TOF$_s$ / min^{-1}
Ir/SiO$_2$	0	0	-	-	5.7
	0.25	0.7	99.6	0.4	
	0.5	1.5	99.3	0.7	
Ni-Ir/SiO$_2$-1	0	0	-	-	38
	0.25	4.4	98.2	1.8	
	0.5	8.9	98.3	1.7	
Ni/SiO$_2$	0	0	-	-	0.1
	13	0.3	93.1	6.9	
	24	0.5	91.4	8.6	

Reaction conditions: catalyst 20 mg, 2-octene 10 mmol, methanol 5 g, H_2 8 MPa, 303 K.

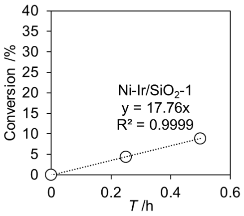

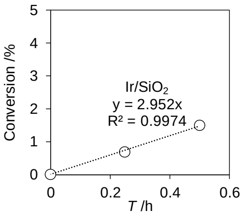

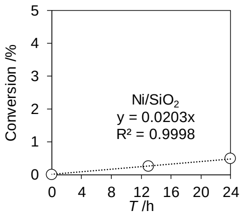

(D) Hydrogenation of ethylbenzene

Catalyst	*t* /h	Conv. /%	Sel./% Ethylcyclohexane	Sel./% 1-Ethylcyclohexene	TOF$_s$ / min^{-1}
Ir/SiO$_2$	0	0	-	-	0.31
	2	0.8	85.0	15.0	
	4	1.5	85.8	14.2	
Ni-Ir/SiO$_2$-1	0	0	-	-	0.17
	2	0.6	60.2	39.8	
	4	1.1	61.5	38.5	
Ni/SiO$_2$	0	0	-	-	
	2	<0.1	-	-	
	4	<0.1	-	-	

Reaction conditions: catalyst 20 mg, ethylbenzene 5 mmol, methanol 3 g, H_2 8 MPa, 353 K.

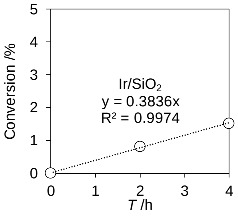

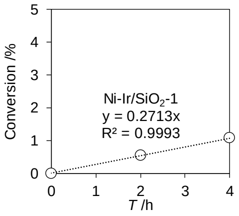

Table S8 Effect of stirring speed in styrene hydrogenation with Ni-Ir/SiO_2-1 catalyst

Stirring speed/ rpm	Conv. /%	Selectivity /%		
		Ethylbenzene	Ethylcyclohexane	Others[a]
300	38.1	>99.9	<0.1	<0.1
500	47.8	>99.9	<0.1	<0.1
700	48.9	>99.9	<0.1	<0.1

Reaction conditions: Ni-Ir/SiO_2-1 20 mg, styrene 200 mmol, methanol 30 g, H_2 8 MPa, 303 K, 0.5 h.

[a] Others include 1-ethylcyclohexene and other partial hydrogenation products of styrene hydrogenation.

Table S9. BET surface areas of Ni-Ir/SiO_2-1 and Ni-Ir/SiO_2-1 after reaction

Catalyst	BET surface area /m^2 g^{-1}
Ni-Ir/SiO_2-1	440
Ni-Ir/SiO_2-1 after reaction[a]	430

[a] Reaction conditions: Ni-Ir/SiO_2-1 20 mg, styrene 200 mmol, methanol 30 g, H_2 8 MPa, 303 K, 0.5 h.

6. References

1. J. W. Cook Jr and D. E. Sayers. *J. Appl. Phys.,* 1981, **52**, 5024-5031.

2. (a) K. Okumura, S. Matsumoto, N. Nishiaki and M. Niwa, *Appl.Catal., B,* 2003, **40**, 151-159; (b) K. Okumura, J. Amano, N. Yasunobu and M. Niwa, *J. Phys. Chem. B,* 2000, **104**, 1050-1057.

3. A. L. Ankudinov, B. Ravel, J. J. Rehr and S. D. Conradson, *Phys. Rev. B,* 1998, **58**, 7565-7576.

4. K. Tomishige, K. Asakura and Y. Iwasawa, *J. Catal.,* 1994, **149**, 70-80.